

Spin-Wave Resonance in Three-Layer NiFe/Dy_xCo_{1-x}/NiFe Films as a Method for Detecting Structural Inhomogeneities in Amorphous Dy_xCo_{1-x} Layers

R. S. Iskhakov^{1,*}, V. A. Seredkin^{1,2}, S. V. Stolyar¹,
L. A. Chekanova¹, and V. Yu. Yakovchuk¹

¹ Kirenskiĭ Institute of Physics, Siberian Division, Russian Academy of Sciences,
Akademgorodok, Krasnoyarsk, 660036 Russia

* e-mail: rauf@iph.krasn.ru

² Krasnoyarsk State University, Krasnoyarsk, 660041 Russia

Received October 21, 2002

The standing spin-wave spectrum was studied by spin-wave resonance in three-layer Ni₈₀Fe₂₀/Dy_xCo_{1-x}/Ni₈₀Fe₂₀ films with an amorphous interlayer of DyCo alloy in the region of compensation compositions. It is shown that the spin-wave resonance (SWR) spectrum in the geometry $\mathbf{k} \parallel M$ is observed only for a planar system with a DyCo layer of precompensation composition. In the $\mathbf{k} \perp M$ geometry, the SWR spectrum was observed for the DyCo systems with both pre- and postcompensation compositions. The exchange stiffness was analyzed as a function of the DyCo layer thickness to formulate a model of microheterophase structure for amorphous DyCo alloys in the compensation region, where the magnetic microstructure accounts for the dynamic and static magnetic characteristics of these materials. © 2002 MAIK "Nauka/Interperiodica".

PACS numbers: 76.50.+g; 75.30.Ds; 75.70.-i

Amorphous RE(Dy, Gd, Tb)–TM(Fe, Co) alloys prepared as solid solutions in a broad concentration range are the brightest representatives of a class of amorphous ferrimagnets. The magnetization of these alloys is the sum of antiparallel magnetizations of the RE and TM sublattices. For this reason, the magnetization in these materials becomes zero at a certain compensation temperature (T_{comp}) or composition (x_{comp}). These materials, when prepared as films with near-compensation compositions, are ordinarily used as media for ultrahigh-density thermomagnetic recording [1]. In these films, the coercive force has a sharp maximum at the points T_{comp} (or x_{comp}). A deviation of only several degrees from T_{comp} (or of 2–3 at. % from x_{comp}) is sufficient for the coercive force to decrease by several times. The magnetic and atomic structures of these alloys were extensively studied in [2]. However, some of their properties, e.g., dynamic properties, are still poorly understood. For instance, studies of these films by ferromagnetic resonance (FMR) show that the FMR line width increases as the film composition (temperature) approaches x_{comp} (T_{comp}) and that no electromagnetic microwave absorption is observed (note that such behavior of the FMR parameters is common to all ferrimagnetic materials [3]).

In this work, we report the results of studying the dynamic magnetic properties of three-layer NiFe/Dy_xCo_{1-x}/NiFe films, in which the amorphous

RE–TM layer is prepared in the region of compensation compositions.

It was established in our experiments that, first, a uniform alternating magnetic field excites standing spin waves in such a three-layer planar composite system. This gives evidence for the exchange interaction between the ferri- and ferromagnetic layers. Second, analysis of the dependence of effective spin-wave stiffness of such a system on the thickness of the ferrimagnetic layer allowed an indirect (but reliable) conclusion to be drawn about some features of the real magnetic and chemical structures of DyCo alloy films with compensation composition.

SAMPLE PREPARATION AND EXPERIMENTAL TECHNIQUE

Three-layer exchange-coupled Ni₈₀Fe₂₀/Dy_xCo_{1-x}/Ni₈₀Fe₂₀ films were prepared by thermal evaporation in a vacuum of 3×10^{-6} torr by sequential deposition of NiFe and DyCo layers on a cover glass substrate from three independent evaporators with ring cathodes. The thicknesses of the Permalloy layers in the planar system were $d_{\text{NiFe}} = 1100$ Å, and the thickness of the Dy_xCo_{1-x} layer was varied in the range from 100 to 800 Å. Single-layer 3000-Å-thick films of Ni₈₀Fe₂₀ Permalloy and single-layer 700-Å-thick Dy_xCo_{1-x} films were used as reference samples. The film thicknesses and chemical compositions were monitored by X-ray spectroscopic

analysis. The amorphous state of the DyCo layer was monitored by electron microscopy. The magneto-optical Kerr effect in fields up to 15 kOe was used as a test method for determining the pre-, post-, and compensation compositions of this layer. The same method (by studying the magneto-optical hysteresis loops at both the outer and inner surfaces of the DyCo layer) was used to establish that the DyCo films were compositionally homogeneous across their width (this was subsequently confirmed by Auger spectroscopy) and had perpendicular anisotropy. In our case, the room-temperature compensation composition was Dy₂₂Co₇₈. Two groups of planar structures were prepared: Ni₈₀Fe₂₀/Dy₂₀Co₈₀/Ni₈₀Fe₂₀ and Ni₈₀Fe₂₀/Dy₂₄Co₇₆/Ni₈₀Fe₂₀. Although the chosen compositions of the ferrimagnetic layer are on opposite sides of x_{comp} , they have close total saturation magnetizations $M_s \approx 80$ G, coercive forces $H_c \approx 4\text{--}5$ kOe, and perpendicular magnetic anisotropies $K_{\perp} \approx 3 \times 10^5$ erg/cm³.

The spin-wave resonance (SWR) spectra of the planar NiFe/Dy_xCo_{1-x}/NiFe structures, single-layer NiFe films, and DyCo films were studied on a standard X-band spectrometer with the cavity fundamental frequency $f = 9.2$ GHz at room temperature. The films were placed at the antinode of an alternating magnetic field in the cavity and magnetized in two geometries (either perpendicular or parallel to the surface). In the first geometry, the resonance fields of SWR peaks (in ferromagnetic films) are known to satisfy the equation

$$H_n = \frac{\omega}{\gamma} + 4\pi M - \eta_{\text{eff}} \mathbf{k}_n^2, \quad \mathbf{k} \parallel M, \quad (1)$$

and, in the second geometry, the equation

$$H_n = \{[(\omega/\gamma)^2 + (2\pi M)^2]^{1/2} - 2\pi M\} - \eta_{\text{eff}} \mathbf{k}_n^2, \quad \mathbf{k} \perp M, \quad (2)$$

where $\omega = 2\pi f$ is the frequency, γ is the gyromagnetic ratio, $\eta_{\text{eff}} = 2A/M$ is the spin-wave stiffness depending on the exchange interaction constant A , M is the magnetization, and $k_n = (\pi/d)n$ ($n = 1, 2, 3, \dots$ and d is the film thickness) is the wave vector of the n th mode in the SWR spectrum.

An important point is that the effective exchange stiffness η_{eff} , calculated by formula

$$\eta_{\text{eff}} = \frac{H_1 - H_n}{n^2 - 1} \left(\frac{d}{\pi}\right)^2, \quad (3)$$

is independent of the geometry of SWR experiment and must have the same value when recording the SWR peaks in both $\mathbf{k} \parallel M$ and $\mathbf{k} \perp M$ geometries. Indeed, the SWR spectra for the reference single-layer 3000-Å Ni₈₀Fe₂₀ films were recorded in both geometries: $\mathbf{k} \parallel M$ (14 peaks, including the surface peak) and $\mathbf{k} \perp M$ (5 peaks) (Fig. 1). Nevertheless, the η_{eff} values calculated by Eq. (3) proved to be nearly the same, with a

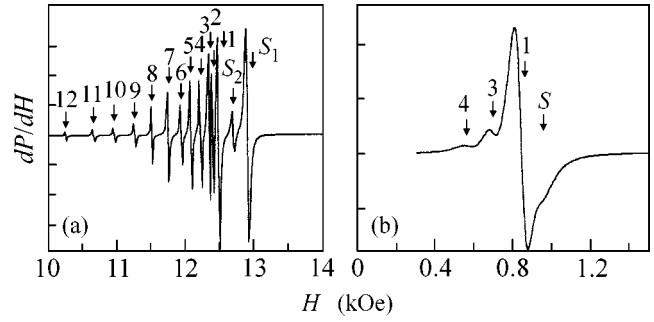


Fig. 1. SWR spectra of the reference Ni₈₀Fe₂₀ films in the dP/dH - H coordinates: (a) $\mathbf{k} \parallel M$ and (b) $\mathbf{k} \perp M$ (S indicates the surface modes and 1, 2, 3, ... label the bulk modes).

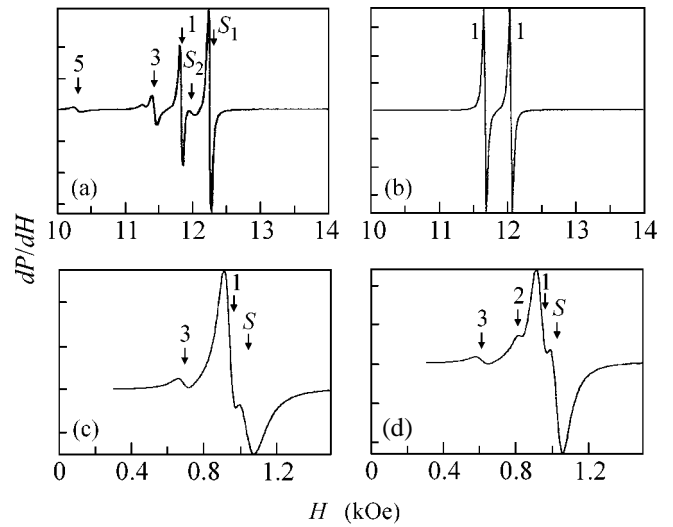


Fig. 2. SWR spectra of the three-layer Ni₈₀Fe₂₀/Dy_xCo_{1-x}/Ni₈₀Fe₂₀ films with a DyCo layer of (a, c) precompensation and (b, d) postcompensation composition in two geometries: (a, b) $\mathbf{k} \parallel M$ and (c, d) $\mathbf{k} \perp M$.

good accuracy, for both cases and equal to $\eta_{\text{eff}} \approx 2.5 \times 10^{-9}$ Oe cm² (this value is consistent with the literature data [4]). No SWR absorption was observed for the reference Dy₂₀Co₈₀, Dy₂₂Co₇₈, or Dy₂₄Co₇₆ films.

RESULTS AND DISCUSSION

Figure 2 shows the absorption spectra of the three-layer NiFe/Dy_xCo_{1-x}/NiFe films studied. The SWR spectrum of the planar Ni₈₀Fe₂₀/Dy₂₀Co₈₀/Ni₈₀Fe₂₀ system in the $\mathbf{k} \parallel M$ geometry is given in Fig. 2a, and the SWR spectrum of Ni₈₀Fe₂₀/Dy₂₄Co₇₆/Ni₈₀Fe₂₀ in the same geometry is given in Fig. 2b. The spectra are essentially different; in a planar system with the DyCo interlayer of precompensation composition, spin waves are excited, whereas, in a planar system with the DyCo

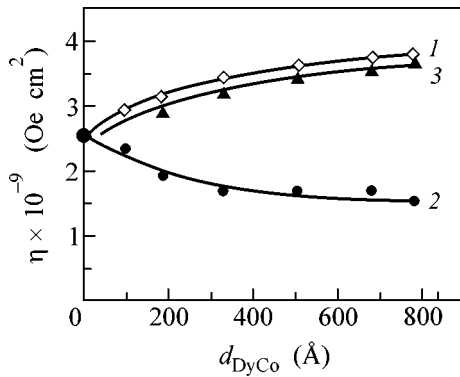


Fig. 3. Dependence of the effective spin-wave stiffness η_{eff} of the three-layer films on the thickness of the DyCo layer: (curve 1) $\eta^{(\mathbf{k} \parallel M)}$ for $\text{Ni}_{80}\text{Fe}_{20}/\text{Dy}_{20}\text{Co}_{80}/\text{Ni}_{80}\text{Fe}_{20}$, (curve 2) $\eta^{(\mathbf{k} \perp M)}$ for $\text{Ni}_{80}\text{Fe}_{20}/\text{Dy}_{20}\text{Co}_{80}/\text{Ni}_{80}\text{Fe}_{20}$, and (curve 3) $\eta^{(\mathbf{k} \perp M)}$ for $\text{Ni}_{80}\text{Fe}_{20}/\text{Dy}_{24}\text{Co}_{76}/\text{Ni}_{80}\text{Fe}_{20}$.

interlayer of postcompensation composition, the spectrum is a superposition of the FMR spectra of the two ferromagnetic NiFe layers. Such a sizable distinction is caused by the exchange interaction between the layers and by the orientation of magnetization of the Co sublattice in the DyCo layer about the external magnetic field. Indeed, for a three-layer system with the interlayer of precompensation composition in the geometry of our experiment, the saturation magnetization vectors of the NiFe layers and the vectors of the overall DyCo magnetization and the magnetization of the Co sublattice are parallel to the external magnetic field H . Owing to the exchange interaction between the magnetic moments of transition metals, the Co magnetic moments are involved in the formation of coherent standing spin waves by microwave fields. In this case, standing waves with different n are sequentially excited upon varying H (Fig. 2a). At the same time, the configuration of the magnetization vectors in a three-layer system with the postcompensation DyCo interlayer is different. The magnetization vector of the Co sublattice in DyCo and the saturation magnetization vectors of the NiFe layers are antiparallel in the saturating fields H . As a result, due to the same exchange interaction, the spectrum of this system is an FMR doublet (Fig. 2b).

Unexpectedly, SWR-type absorption was observed in the $\mathbf{k} \perp M$ geometry (the external field is parallel to the film planes) for the planar systems with both pre- and postcompensation DyCo interlayers (Figs. 2c and 2d, respectively). The point is that the external field H (~ 1 kOe) in this geometry is appreciably weaker than the coercive force of the ferrimagnetic DyCo layer ($H_c \approx 4-5$ kOe). Consequently, this field cannot change the orientation of the total magnetization in the DyCo layer (as also the orientations of sublattice magnetizations). This became clear after the parameters of SWR spectra were changed by varying the thickness of the DyCo interlayer from 100 to 800 Å.

Figure 3 presents the effective exchange stiffness η_{eff} as a function of the thickness of the DyCo layer, as calculated by formula (3) from the experimental SWR spectra given by Eq. (1) for the planar $\text{Ni}_{80}\text{Fe}_{20}/\text{Dy}_{20}\text{Co}_{80}/\text{Ni}_{80}\text{Fe}_{20}$ system in the $\mathbf{k} \parallel M$ geometry (curve 1) and by Eq. (2) for the $\text{Ni}_{80}\text{Fe}_{20}/\text{Dy}_{20}\text{Co}_{80}/\text{Ni}_{80}\text{Fe}_{20}$ and $\text{Ni}_{80}\text{Fe}_{20}/\text{Dy}_{24}\text{Co}_{76}/\text{Ni}_{80}\text{Fe}_{20}$ systems in the $\mathbf{k} \perp M$ geometry (curves 2 and 3, respectively). In this figure, the exchange stiffness η_{eff} of the reference NiFe film is plotted on the ordinate axis (The formation of an effective exchange stiffness η_{eff} from the partial exchange stiffnesses η_i of the individual layers in a three-layer system is not discussed in this work).

One can see that the value of exchange stiffness η_{eff} of the $\text{Ni}_{80}\text{Fe}_{20}/\text{Dy}_{20}\text{Co}_{80}/\text{Ni}_{80}\text{Fe}_{20}$ system depends on the geometry of the SWR experiment; the calculated ratio $\eta_{\text{eff}}(\mathbf{k} \parallel M)$ to $\eta_{\text{eff}}(\mathbf{k} \perp M)$ is as high as two or even higher (curves 1, 2), which far exceeds the experimental error ($\sim 10\%$). At the same time, one can see that the values of η_{eff} measured for the $\text{Ni}_{80}\text{Fe}_{20}/\text{Dy}_{24}\text{Co}_{76}/\text{Ni}_{80}\text{Fe}_{20}$ system in the $\mathbf{k} \perp M$ geometry (curve 3) are close to their values in the system with the $\text{Dy}_{20}\text{Co}_{80}$ interlayer in the $\mathbf{k} \parallel M$ geometry. On the assumption that the exchange stiffness of a ferromagnetic film does not depend on the SWR geometry, one arrives at the conclusion that η_{eff} for curves 1 and 3 (Fig. 3) characterize the same magnetic material, while η_{eff} for curve 2 (Fig. 3) corresponds to a different magnetic material.

In our opinion, these results reflect the fundamental property of the amorphous state, namely, the intrinsic structural (fluctuative) inhomogeneity of amorphous alloys. Amorphous alloys are known to contain chemical (phase) nanoscale inhomogeneities. In particular, these inhomogeneities in amorphous ferromagnetic alloys cause fluctuations of exchange interaction and saturation magnetization, which was repeatedly detected experimentally (including the SWR method [5–8]). The magnitude of concentration fluctuations in these alloys can be as high as several atomic percent of mean concentration. This is the key factor that underlies the specific behavior of DyCo alloys in the compensation region. It is natural to introduce the notion of two magnetic phases for this alloy: the Φ_1 phase, for which the inequality $M_{\text{Co}} > M_{\text{Dy}}$ is satisfied locally and integrally, and the phase Φ_2 , for which the inequality $M_{\text{Dy}} > M_{\text{Co}}$ is satisfied on the micro- and macrolevel. In the range of concentrations $x \ll x_{\text{comp}}$ or $x \gg x_{\text{comp}}$, the magnetic structure of the DyCo alloy is uniquely related to either Φ_1 or Φ_2 . A basically different situation occurs in the region $x \approx x_{\text{comp}}$ under the condition that Δ_x falls within the range of fluctuations of local concentrations. In this case, the compensation point x_{comp} is determined from the requirement that the volumes of chaotically mixed Φ_1 and Φ_2 phases be the same. Then the pre- and postcompensation DyCo alloys are defined by

the inequalities $V_{\Phi_1} > V_{\Phi_2}$, $V_{\Phi_1} < V_{\Phi_2}$, respectively. According to simple estimates within the framework of percolation theory, one can state that the percolation near x_{comp} occurs through both Φ_1 and Φ_2 up to the concentrations x^* for which the condition $V_{\Phi_1} \approx 2V_{\Phi_2}$ or $2V_{\Phi_1} \approx V_{\Phi_2}$ is met.

The results of our experiment can naturally be interpreted in terms of the scheme proposed in Fig. 4 (the arrows in this figure indicate the possible magnetization orientations for 3d metals and the magnetization profile across the thickness of a three-layer film in the first SWR mode). Figure 4a describes the experimental situation presented in Fig. 2a. In Fig. 4a, Φ_1 and Φ_2 denote, respectively, the matrix and impurity phases in the $\text{Dy}_{20}\text{Co}_{80}$ layer. The magnetization M_{Co} in phase Φ_1 is aligned with both the external and perpendicular anisotropy fields. Due to the exchange interaction between transition metals, the magnetization of M_{Co} in the impurity phase Φ_2 should have the in-plane component in this case. For this reason, the coherent spin wave in the three-layer $\text{Ni}_{80}\text{Fe}_{20}/\text{Dy}_{20}\text{Co}_{80}/\text{Ni}_{80}\text{Fe}_{20}$ system propagates in the $\mathbf{k} \parallel M$ geometry through the phase Φ_1 , and, in the $\mathbf{k} \perp M$ geometry, through the phase Φ_2 (Figs. 2c and 4c). Then the difference in the η_{eff} values for curves 1 and 2 in Fig. 3 is physically understandable, because the effective thickness in this case is contributed by the partial stiffnesses η_i of, in fact, different magnetic materials. The situation is the reverse for the $\text{Ni}_{80}\text{Fe}_{20}/\text{Dy}_{24}\text{Co}_{76}/\text{Ni}_{80}\text{Fe}_{20}$ system, where Φ_2 and Φ_1 are the matrix and impurity phases, respectively. In this case, the magnetization M_{Dy} of the Φ_2 phase is aligned with the external field in the SWR geometry ($\mathbf{k} \parallel M$), while the magnetization M_{Co} of this phase is antialigned with both external field and NiFe magnetizations. In such a situation, the coherent spin wave can be excited only in the NiFe layers (Figs. 2b and 4b). However, the magnetization M_{Co} of the impurity phase can contain the in-plane component. For this reason, the coherent spin wave in the three-layer $\text{Ni}_{80}\text{Fe}_{20}/\text{Dy}_{24}\text{Co}_{76}/\text{Ni}_{80}\text{Fe}_{20}$ system can propagate in the $\mathbf{k} \perp M$ geometry through the impurity phase Φ_1 (Figs. 2d and 4d). This explains the agreement between the η_{eff} values for curves 1 and 3 in Fig. 3.

Thus, the SWR studies of the three-layer planar $\text{Ni}_{80}\text{Fe}_{20}/\text{Dy}_x\text{Co}_{1-x}/\text{Ni}_{80}\text{Fe}_{20}$ systems containing amorphous DyCo interlayer in the region of compensation compositions enable one not only to judge indirectly

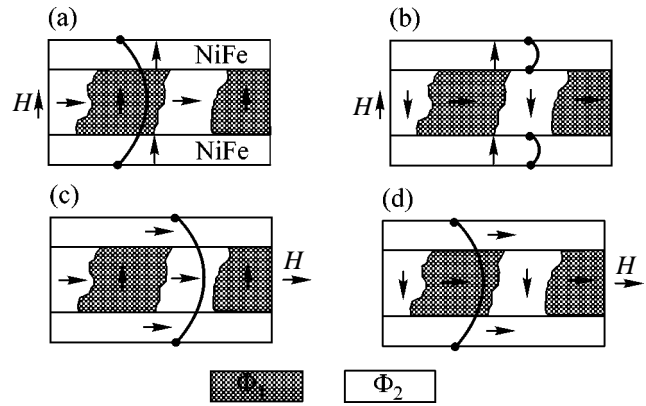


Fig. 4. Configuration of the magnetization vectors for 3d metals in the three-layer films and the first standing-wave mode: (a, c) precompensation and (b, d) postcompensation DyCo compositions.

(though, in our opinion, reliably) the inhomogeneous structure of these amorphous DyCo films but also propose a model of microheterophase organization of this industrially important class of magnetic materials.

This work was supported by the Russian Foundation for Basic Research, project no. 02-02-97717.

REFERENCES

1. R. W. Chantrell, A. Lyberatos, M. El-Hilo, and K. O. Grady, *J. Appl. Phys.* **76**, 6407 (1994).
2. K. H. J. Buschow, in *Ferromagnetic Materials*, Ed. by E. P. Wohlfarth and K. H. J. Buschow (Elsevier, New York, 1988), Vol. 4.
3. A. G. Gurevich, *Magnetic Resonance in Ferrites and Antiferromagnets* (Nauka, Moscow, 1973).
4. G. I. Rusov, *Fiz. Tverd. Tela (Leningrad)* **9**, 196 (1967) [*Sov. Phys. Solid State* **9**, 146 (1967)].
5. V. A. Ignatchenko, R. S. Iskhakov, L. A. Chekanova, and N. S. Chistyakov, *Zh. Éksp. Teor. Fiz.* **75**, 876 (1978) [*Sov. Phys. JETP* **48**, 328 (1978)].
6. R. S. Iskhakov, M. M. Brushtunov, A. S. Chekanov, *et al.*, *Fiz. Met. Metalloved.* **79**, 122 (1995).
7. R. S. Iskhakov, S. V. Stolyar, L. A. Chekanova, and V. S. Zhigalov, *Fiz. Tverd. Tela (St. Petersburg)* **43**, 1072 (2001) [*Phys. Solid State* **43**, 1108 (2001)].
8. R. S. Iskhakov, D. E. Prokof'ev, L. A. Chekanova, and V. S. Zhigalov, *Pis'ma Zh. Tekh. Fiz.* **27** (8), 81 (2001) [*Tech. Phys. Lett.* **27**, 344 (2001)].

Translated by V. Sakun